COMMISSIONS G1 AND G4 OF THE IAU
INFORMATION BULLETIN ON VARIABLE STARS
Volume 63 Number 6224 DOI: 10.22444/IBVS.6224

Konkoly Observatory
Budapest
11 December 2017

HU ISSN 0374 – 0676

V500 Cyg – A CLASSICAL ALGOL

NELSON, ROBERT H.[1,2,3]

[1] Mountain Ash Observatory, 1393 Garvin Street, Prince George, BC, Canada, V2M 3Z1, bob.nelson@shaw.ca

[2] Guest investigator, Dominion Astrophysical Observatory, Herzberg Institute of Astrophysics, National Research Council of Canada

[3] Desert Blooms Observatory, Benson AZ, 31°56.454′N, 110°15.450′W

The discoverer of the variability of V500 Cyg (AN 1939.0081; TYC 2693–139–1) appears to be undocumented. The first available reference (in the GCVS and SIMBAD) is Whitney (1959) who provided revised elements, three new eclipse timings, and notes regarding a companion separated by 0.3′. Since then, there have been numerous eclipse timings published, but no light curve or analysis.

In order to rectify this lack, the author first secured, in the autumns of 2010, 2013, 2014, and 2015, a total of eight medium resolution (R $\sim$ 10000 on average) spectra of V500 Cyg at the Dominion Astrophysical Observatory (DAO) in Victoria, British Columbia, Canada using the Cassegrain spectrograph attached to the 1.85 m Plaskett Telescope. He used the 21181 configuration and a grating with 1800 lines/mm, blazed at 5000 Å, and giving a reciprocal linear dispersion of 10 Å/mm in the first order. The wavelengths ranged from 5000 to 5260 Å, approximately. A log of observations is given in Table 1 and an eclipse timing diagram, in Figure 9 later in the paper. The latter was used to derive the following elements, used for both radial velocity (RV) and photometric phasing:

$$\text{JD (Hel) Min I} = 2457914.8640(49) + 0.9242233(2)E \quad (1)$$

where the quantities in brackets are the standard errors of the preceding quantities in units of the last digit.

Frame reduction was performed by software RaVeRe (Nelson 2013). See Nelson (2010) and Nelson et al. (2014) for further details. The normalized spectra are reproduced in Fig. 1, sorted by phase (the vertical scale is arbitrary). Note towards the right the strong neutral iron lines (at 5167.487 and 5171.595 Å) and the strong neutral magnesium triplet (at 5167.33, 5172.68, and 5183.61 Å).

Radial velocities were determined using the Rucinski broadening functions (Rucinski, 2004, Nelson, 2010) as implemented in software Broad25 (Nelson, 2013). See Nelson et al. (2014) for further details. An Excel worksheet with built-in macros (written by him) was used to do the necessary radial velocity conversions to geocentric and back to heliocentric values (Nelson 2014). The resulting RV determinations are also presented in Table 1 (along with standard errors in units of the last digits, enclosed in brackets). The mean rms errors for RV_1 and RV_2 are 3.8 and 11.3 km/s, respectively, and the overall

Table 1: Log of DAO observations

DAO Image #	Mid Time (HJD−2400000)	Exposure (sec)	Phase at Mid−exp	V1 (km/s)	V2 (km/s)
10-17392	55474.7097	3600	0.778	77.4 (2.8)	−215.3 (14.8)
13-09641	56544.8987	3600	0.712	74.1 (4.2)	−225.2 (10.8)
12-24533	56912.6665	3600	0.633	42.3 (1.3)	−196.3 (0.9)
15-13142	57295.8492	3600	0.232	−123.5 (4.8)	159.9 (10.7)
15-13144	57295.8926	3600	0.279	−126.1 (5.0)	174.0 (16.5)
15-13176	57296.8290	3600	0.292	−120.4 (4.6)	163.3 (13.5)
15-13238	57298.7427	3600	0.363	−94.6 (2.6)	104.2 (7.0)
15-13265	57299.6278	3600	0.321	−113.8 (4.8)	134.6 (16.3)

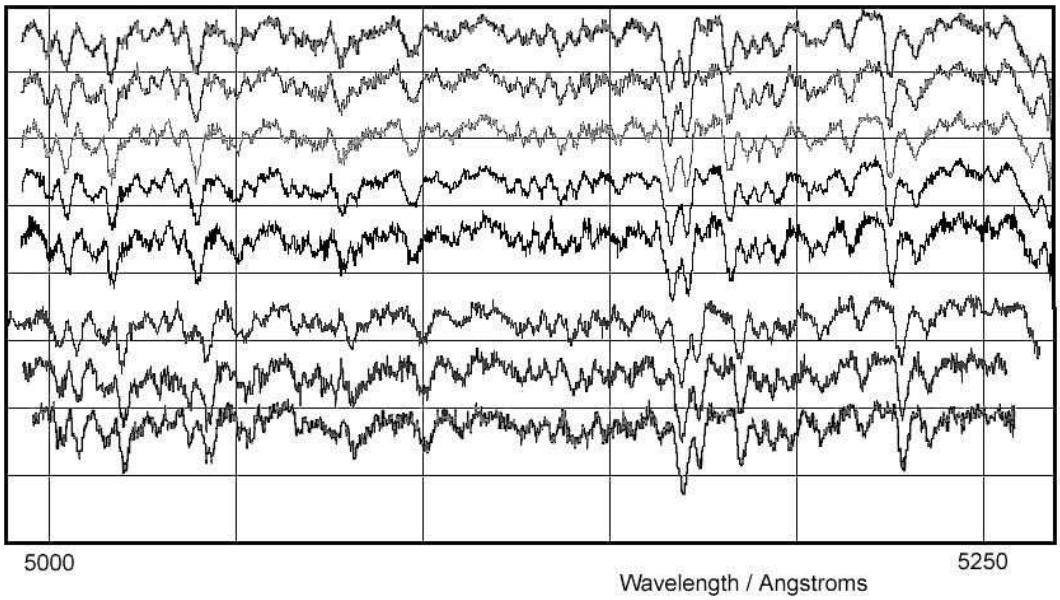

Figure 1. V500 Cyg spectra at phases 0.232, 0.279, 0.292, 0.321, 0.363, 0.633, 0.712, 0.778 (from top to bottom). Each has been shifted vertically for clarity. The vertical scale is arbitrary.

rms deviation from the (sinusoidal) curves of best fit is 9.7 km/s. The best fit yielded the values $K_1 = 98.6(2.7)$ km/s, $K_2 = 196.8(4.9)$ km/s and $V_\gamma = -129.1(2.2)$ km/s, and thus a mass ratio $q_{\rm sp} = K_1/K_2 = M_2/M_1 = 0.50(1)$.

Representative broadening functions, at phases 0.232 and 0.778 are depicted in Figs. 2 and 3, respectively (the vertical scale is arbitrary). Smoothing by a Gaussian filter is routinely done in order to centroid the peak values for determining the radial velocities.

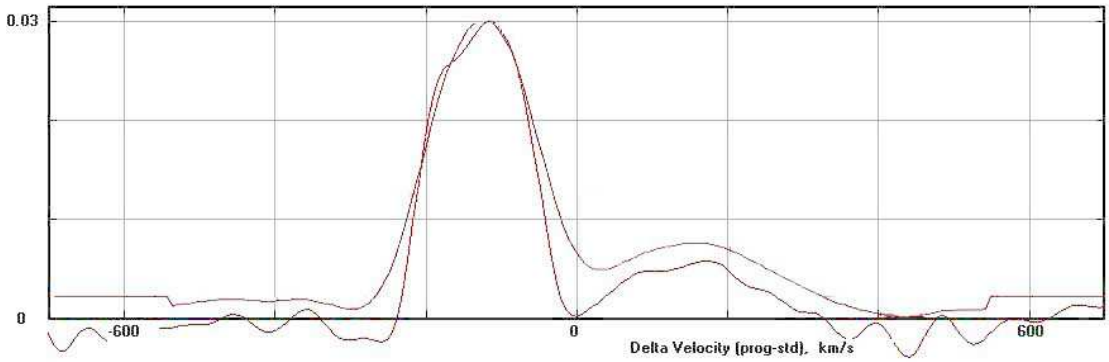

Figure 2. Broadening functions at phase 0.232–smoothed and unsmoothed.

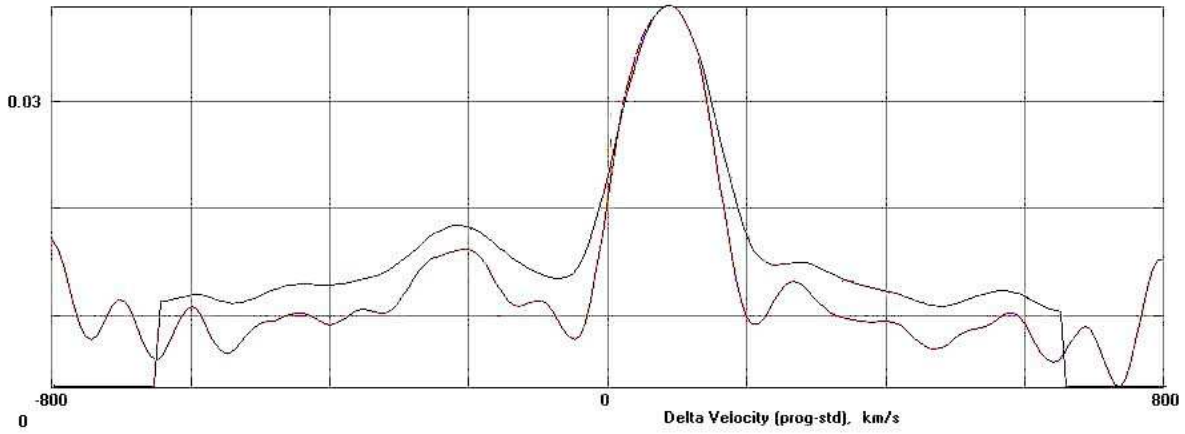

Figure 3. Broadening functions at phase 0.778–smoothed and unsmoothed.

During twelve nights in 2017, May 24 -June 14, the author took a total of 198 frames in V, 197 in $R_{\rm C}$ (Cousins) and 199 in the $I_{\rm C}$ (Cousins) band at the newly-opened Desert Blooms Observatory, jointly owned by the author and Dr. Kevin B. Alton. Hosted at the San Pedro Observatory complex located near Benson, Arizona, the telescope is operated remotely. It consists of a Software Bisque Taurus 400 equatorial fork mount, a Meade LX-200 40 cm Schmidt-Cassegrain optical assembly operating at f/7, a SBIG STT-1603 XME CCD camera (with a field of view $11' \times 18'$), and a filter wheel with the usual B, V, $R_{\rm C}$, and $I_{\rm C}$ filters. For unattended operation, automatic focusing is required owing to the large temperature changes throughout the night (typically +35 °C to +10 °C in late spring).

Table 2: Details of variable, comparison and check stars.

Object	GSC	RA (J2000)	Dec (J2000)	V (mag)	$B-V$ (mag)
Variable	2693-0139	$20^{\rm h}24^{\rm m}40\overset{\rm s}{.}379$	$+34°57'05\overset{''}{.}40$	11.91 (16)	+0.25 (21)
Comparison	2693-0828	$20^{\rm h}24^{\rm m}39^{\rm s}$	$+34°56'59''$	11.20 (7)	0.22 (9)
Check 1	2693-1630	$20^{\rm h}24^{\rm m}28^{\rm s}$	$+34°55'45''$	12.1	0.34
Check 2	2693-1230	$20^{\rm h}24^{\rm m}16\overset{\rm s}{.}9528$	$+34°58'39\overset{''}{.}642$	10.91 (7)	+0.73 (14)

Table 3: Limb darkening values from Van Hamme (1993).

Band	x_1	x_2	y_1	y_2
Bol	0.640	0.628	0.242	0.150
V	0.707	0.797	0.278	0.015
$R_{\rm C}$	0.634	0.753	0.286	0.104
$I_{\rm C}$	0.550	0.667	0.276	0.150

Standard reductions were then applied (see Nelson et al. 2014 for more details). The variable, comparison, and check stars are listed in Table 2. The coordinates and magnitudes for V500 Cyg, the comparison, and check 2 are from the Tycho Catalogue, Hog et al. (2000), with magnitudes converted to standard Johnson values using relations due to Henden (2001). For check 1, the V magnitude is from the GSC catalogue and the approximate $B-V$ value is from our photometry. Quantities in brackets are standard errors, in units of the last digit.

The author used the 2003 version of the Wilson-Devinney (WD) light curve and radial velocity analysis program with Kurucz atmospheres (Wilson & Devinney, 1971, Kurucz, 1979, Wilson, 1990, Kallrath & Milone, 1998, Wilson, 1998) as implemented in the Windows front-end software WDwint (Nelson, 2013) to analyze the data. To get started, the spectral type F4–5 (taken from SIMBAD, no reference given; main sequence assumed) was adopted. Interpolated tables from Flower (1996) gave a temperature $T_1 = 6610 \pm 134$ K (T_1 is the mean of the two sub-classes) and $\log g = 4.348 \pm 0.014$. (The quoted errors refer to one spectral sub-class.) An interpolation program by Terrell (1994, available from Nelson 2013) gave the Van Hamme (1993) limb darkening values; and finally, a logarithmic (LD = 2) law for the limb darkening coefficients was selected, appropriate for temperatures < 8500 K (ibid.). The limb darkening coefficients are listed in Table 3. (The values for the second star are based on the later-determined temperature of 4584 K and assumed spectral type of K5.) Convective envelopes for both stars were used, appropriate for cooler stars (hence values gravity exponent $g = 0.32$ and albedo $A = 0.500$ were used for each).

From the GCVS 4 designation (EA/SD) and from the shape of the light curve, mode 5 (classical Algol) mode was used. Later on, mode 2 (detached) was tried but DC adjustments required decreases in potential 2 below the critical value; consequently mode 2 was abandoned.

Convergence using differential corrections (DC) and the method of multiple subsets was reached in a small number of iterations. (See Wilson & Devinney, 1971 and Kallrath & Milone 1998 for an explanation of the method.) The subsets were: (a, V_γ, i, L_1), (T_2, q), and (T_2, Ω_1). However, the visual fit was poor in that the calculated depth of the secondary minimum was too deep. Therefore, in LC mode temperature T_2 was lowered until the fit was satisfactory. Then, switching back to DC mode, temperature T_2 was held constant while all other parameters allowed to vary. Once convergence was obtained, T_2 was again allowed to vary with only small changes indicated.

Table 4: Wilson–Devinney parameters.

WD Quantity	Value	Revised values	error	Unit
Temperature, T_1	6610	6610	[fixed]	K
Temperature, T_2	4584	4594	200	K
$q = m_2/m_1$	0.557	0.554	0.005	—
Potential, Ω_1	3.703	3.690	0.015	—
Potential, Ω_2	2.984	2.978	[fixed]	
Inclination, i	83.06	83.38	0.10	degrees
Semi-major axis a	5.38	5.38	0.12	solar radii
V_γ	−25.3	−25.3	2.6	km/s
Fill-out, f_1	−2.186	−2.177	0.001	
$L_1/(L_1 + L_2)$ (V)	0.8664	0.8664	0.0003	—
$L_1/(L_1 + L_2)$ (R_C	0.8245	0.8245	0.0004	—
$L_1/(L_1 + L_2)$ (I_C)	0.7866	0.7866	0.0006	—
r_1 (pole)	0.3153	0.3153	0.0015	orbital radii
r_1 (point)	0.3377	0.3377	0.0022	orbital radii
r_1 (side)	0.3234	0.3234	0.0017	orbital radii
r_1 (back)	0.3317	0.3317	0.0019	orbital radii
r_2 (pole)	0.3083	0.3083	0.0007	orbital radii
r_2 (point)	0.4402	0.4402	0.0027	orbital radii
r_2 (side)	0.3220	0.3220	0.0007	orbital radii
r_2 (back)	0.3544	0.3544	0.0007	orbital radii
Phase shift	0.0011	0.0016	0.0001	—
$\Sigma\omega^2_{\rm res}$	0.06012	0.03943	—	—

Detailed reflections were tried, with the number of reflections, $n_{\rm ref} = 3$, but there was little–if any–difference in the fit from the simple treatment.

The model is presented in Table 4 (for an explanation of column 3, see below). For the most part, the error estimates are those provided by the WD routines and are known to be under-estimated; however, it is a common practice to quote these values and we do so here. Also, estimating the uncertainties in temperatures T_1 and T_2 is somewhat problematic. A common practice is to quote the temperature difference over–say–one spectral sub-class (assuming that the classification is good to one spectral sub-class, the precision being unknown in this case). In addition, various different calibrations have been made (Cox, 2000, page 388–390 and references therein, and Flower, 1996), and the variations between the various calibrations can be significant. If the classification is ± one sub-class, an uncertainty of ± 200 K to the absolute temperatures of each, would be reasonable. The modelling error in temperature T_2, relative to T_1, is indicated by the WD output to be much smaller, around 9 K.)

The light curve data and the fitted curves are depicted in Figures 4–6. The residuals (in the sense observed-calculated) are also plotted, shifted upwards by 0.25 units.

It is not clear why, in all three light curves, a few points near phase 0.03 (and all from the same night) are deviant, other than possibly due to a passing cloud which could have differentially affected the flux from one of the stars (variable, comparison) compared to the other. In response to a referee's concerns about these errant points, new modelling trials were undertaken with these points deleted. The result was slight differences in the resultant parameters at convergence; these are reported in column 3. The reader will note that, for the most part, these lie inside the estimated (one sigma) confidence intervals and

are therefore not significantly different.

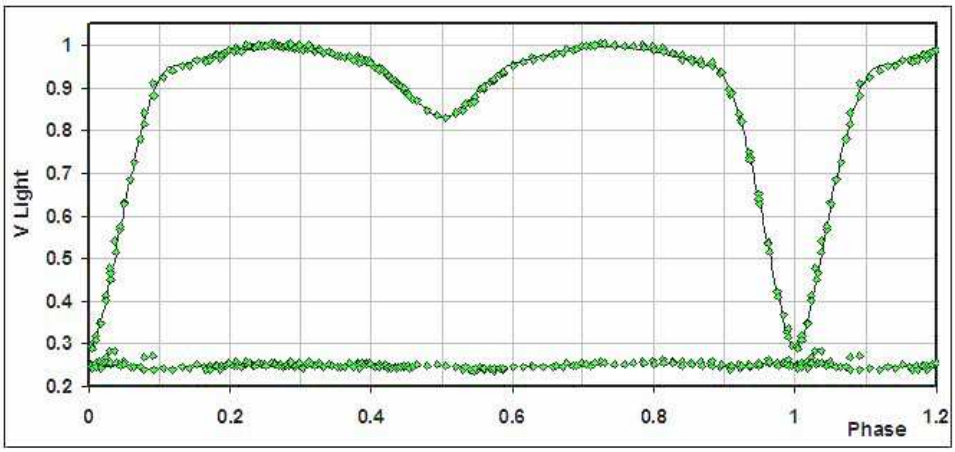

Figure 4. V light curves for V500 Cyg – data, WD fit, and residuals.

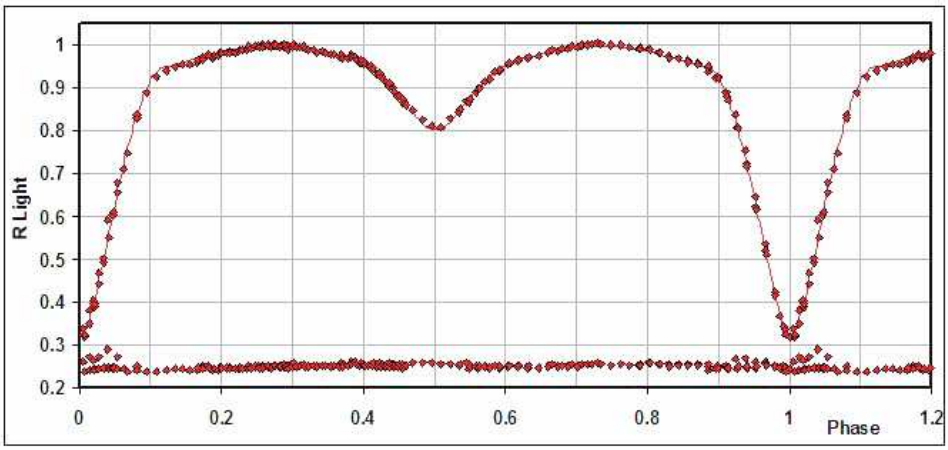

Figure 5. R light curves for V500 Cyg – data, WD fit, and residuals.

The radial velocities are shown in Fig. 7. A three-dimensional representation from Binary Maker 3 (Bradstreet, 1993) is shown in Fig. 8. (The crosses are the centres of mass of the individual stars and of the system as a whole. The ellipses are of the respective centres of mass.)

The WD output fundamental parameters and errors are listed in Table 5. Most of the errors are output or derived estimates from the WD routines. From Kallrath & Milone (1998), the fill-out factor is f = $(\Omega_{\rm I} - \Omega)/(\Omega_{\rm I} - \Omega_{\rm O})$, where Ω is the modified Kopal potential of the system, $\Omega_{\rm I}$ is that of the inner Lagrangian surface, and $\Omega_{\rm O}$, that of the outer Lagrangian surface, was also calculated.

To determine the distance, the analysis proceeded as follows: first the WD routine gave the absolute bolometric magnitudes of each component; these were then converted to the absolute visual (V) magnitudes of both, $M_{\rm V,1}$ and $M_{\rm V,2}$, using the bolometric

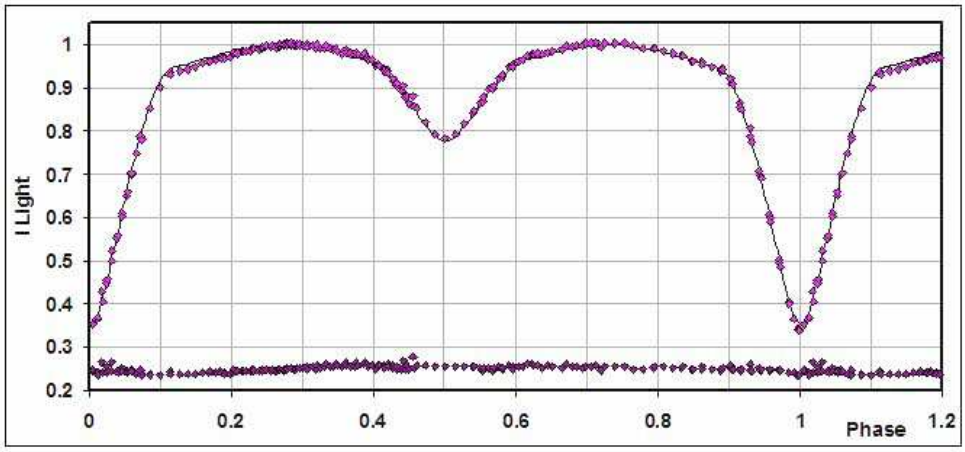

Figure 6. *I* light curves for V500 Cyg – data, WD fit, and residuals.

Table 5: Fundamental parameters.

Quantity	Value	Error	unit
Temperature, T_1	6610	200	K
Temperature, T_2	4584	200	K
Mass, m_1	1.58	0.10	M0
Mass, m_2	0.88	0.04	M0
Radius, R_1	1.74	0.01	R0
Radius, R_2	1.77	0.01	R0
$M_{\rm bol,1}$	3.00	0.02	mag
$M_{\rm bol,2}$	4.55	0.02	mag
$\log g_1$	4.15	0.01	cgs
$\log g_2$	3.88	0.01	cgs
Luminosity, L_1	5.20	0.10	L0
Luminosity, L_2	1.25	0.02	L0
Fill-out factor 1	-2.219	0.010	—
Fill-out factor 2	0	[fixed]	
Distance, r	602	27	pc

corrections BC $= -0.135$ and -0.72 for stars 1 and 2 respectively. The latter were taken from interpolated tables constructed from Cox (2000). The absolute V magnitude was then computed in the usual way, getting $M_V = 2.63 \pm 0.06$ magnitudes. The apparent magnitude in the V passband was $V = 11.93 \pm 0.02$, taken from the Tycho values (Hog et al. 2000) and converted to the Johnson magnitude 11.91 ± 0.02 using relations due to Henden (2001).

Ignoring interstellar absorption, we calculated a preliminary value for the distance $r = 717$ pc from the standard relation:

$$r = 10^{0.2(V - M_V - A_V + 5)} \text{ parsecs} \qquad (2)$$

Galactic extinction was obtained from a model by Amôres & Lépine (2005). The code (available in IDL and converted by the author to a Visual Basic routine) assumes that the interstellar dust is well mixed with the gas, that the Galaxy is axisymmetric, that the gas density in the disk is a function of the Galactic radius and of the distance from

the Galactic plane, and that extinction is proportional to the column density of the gas, Using Galactic coordinates of $l = 74.0787°$ and $b = -1.5709°$ (SIMBAD), and the initial distance estimate of $d = 0.717$ kpc, a value of $A_V = 0.451$ mag was determined, Further iteration of several steps resulted in final values of $A_V = 0.382$ mag and $r = 602$ pc.

The errors were assigned as follows: $\delta M_{\mathrm{bol},1} = \delta M_{\mathrm{bol},2} = 0.02$, $\delta \mathrm{BC}_1 = \delta \mathrm{BC}_2 = 0.09$ (the variation of 1 spectral sub-class), $\delta V = 0.02$, $\delta A_V = 0.02$, all in magnitudes. Combining the errors rigorously (i.e., by adding the variances) yielded an estimated error in r of 27 pc.

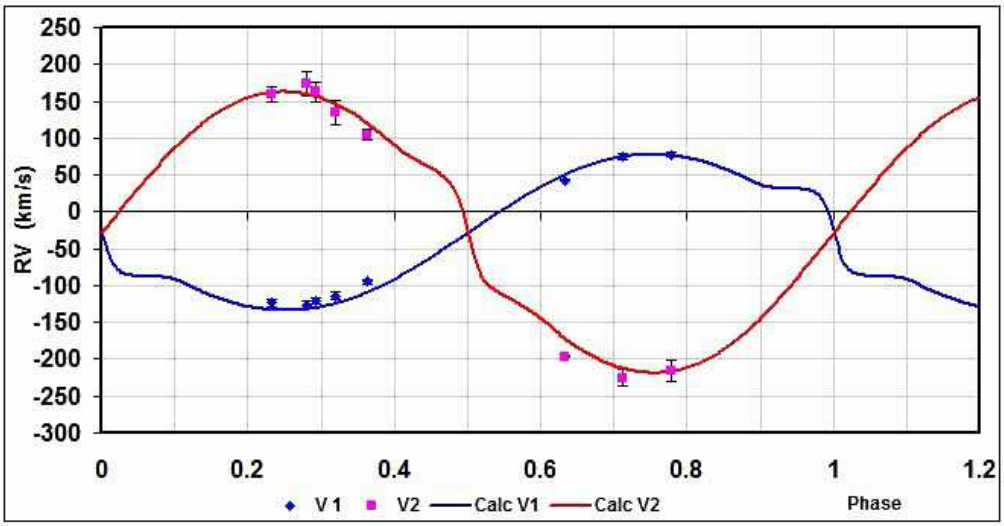

Figure 7. Radial velocity curves for V500 Cyg – data and WD fit.

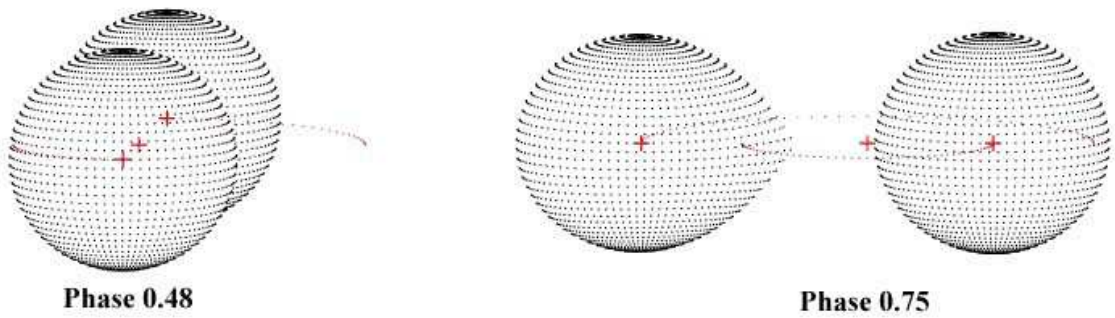

Figure 8. Binary Maker 3 representation of the system – at phases 0.48 and 0.75.

Four new times of minima emerged from the observations; these are reported in Table 6. Each is the mean of three values (one for each filter). Four methods of minimum determination, as implemented in software Minima23 (Nelson 2013), were used: the digital tracing paper method, sliding integrations (Ghedini 1982), curve fitting using five Fourier terms, and Kwee and van Woerden (Kwee & Woerden 1956, Ghedini 1982). Because, in the literature, many (or perhaps most) error estimates can be shown to be low (sometimes unrealistically so), the estimated errors were taken as double the standard deviations of the various determinations.

Table 6: New times of minima for V500 Cyg obtained in this study.

Min (Hel)−2400000	Type	Error (days)
57901.9264	I	0.0002
57908.8590	II	0.0006
57913.9397	I	0.0004
57914.8639	I	0.0009

Some comments regarding the period variation are in order. An eclipse timing difference (O–C) plot using timings from 1988 is depicted in Fig. 9. Although there is considerable scatter, a linear relation over the data collection interval (cycles 28800 to 30770 for the RVs and cycles 31420 to 31440 for the light curve data) is assumed. This yielded a weighted best-fit linear solution and ephemeris of Equation (1) above. (Standard weighting was used: pg = 0.2, vis = 0.1, and PE = CCD = 1. Two nearly identical points lying more than three standard deviations from the curve of best fit were rejected.)

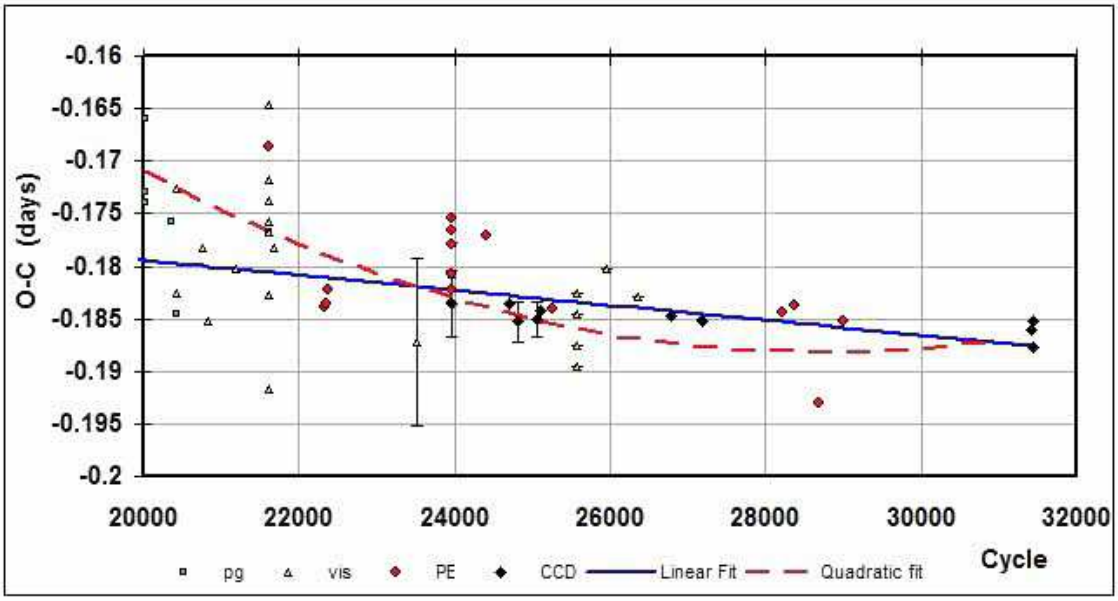

Figure 9. V500 Cyg – eclipse timing (O–C) diagram with linear (solid blue) and quadratic (dashed red) fits for points after cycle 20000 (see equation 1). (Note: pg = photographic; vis = visual; PE = photoelectric; and CCD = charge coupled device.

Also, all the available timing data since the earliest in 1935 (available online at Nelson 2016) are plotted in Fig. 10. There may well be a quadratic relation; the relevant parameters for which are given in Equation 3.

$$\text{JD (Hel) Min I} = 2457914.8651(29) + 0.9242105(5) + 2.1(2) \times 10^{-10} E^2 \qquad (3)$$

However, the quadratic relation does not fit the data since cycle 20000 particularly well (see Fig. 9) and was not used in the analysis. The period behaviour might perhaps be better explained by the light time effect (LiTE; Irwin 1952, 1959) due to a third star. However, due to the obvious scatter in the early photographic data near cycle 0, (due to Wachmann, cited in the O–C Gateway with only the ambiguous reference of AAAN

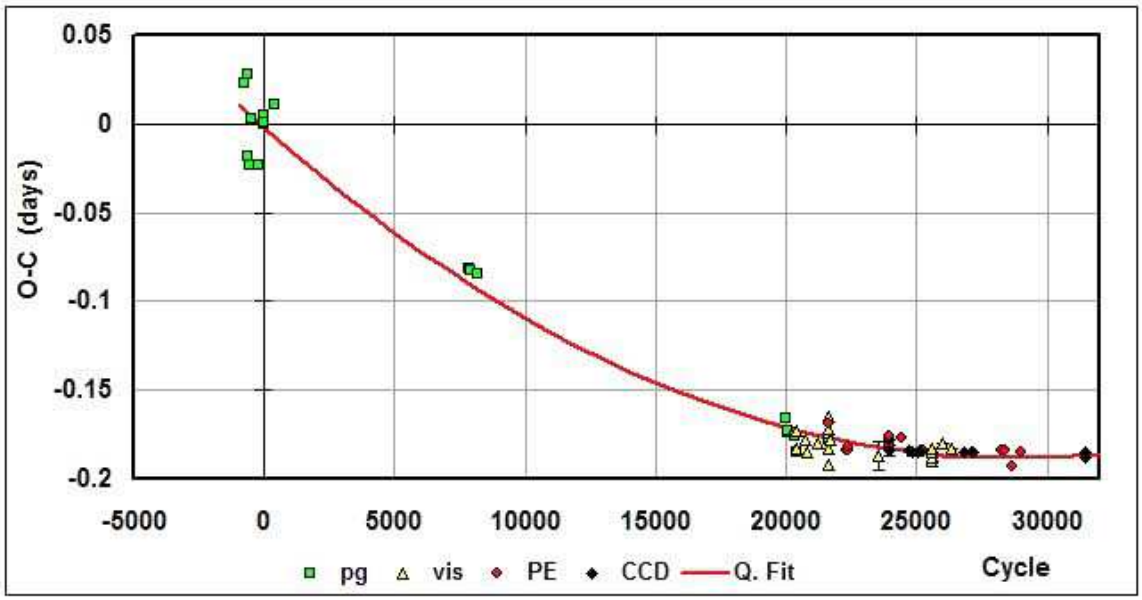

Figure 10. V500 Cyg – eclipse timing (O–C) diagram with a quadratic fit for all available points.

11.5.43), a LiTE analysis does not appear to be justified at this time. High quality data over the coming decades will be required to settle the matter. The reader is referred to Nelson et al. (2014, 2015, 2016) for further discussions on this difficulties encountered in period analysis.

Acknowledgements: It is a pleasure to thank the staff members at the DAO (Dmitry Monin, David Bohlender, and the late Les Saddlmyer) for their usual splendid help and assistance. Many thanks are also due to the San Pedro Observatory resident astronomer/technician Dean Salman for his tireless help. Much use was made of the SIMBAD database during this research.

References:

Amôres, E.B., Lépine, J.R.D., 2005, *AJ*, **130**, 659 DOI
Bradstreet, D.H., 1993, *IAUCB*, **21**, 151 DOI
Cox, A.N., ed, 2000, Allen's Astrophysical Quantities, 4th ed., (Springer, New York, NY) DOI
Flower, P.J., 1996, *ApJ*, **469**, 355 DOI
Ghedini, S., 1982, Software for Photometric Astronomy (Willmann-Bell, Inc.)
Henden, A., 2001, `http://www.tass-survey.org/tass/catalogs/tycho.old.html`
Hog, E., et al., 2000, *A&A*, **355**, L27
Irwin, J.B., 1952, *ApJ*, **116**, 211 DOI
Irwin, J.B., 1959, *AJ*, **64**, 149 DOI
Kallrath, J., Milone, E.F., 1998, Eclipsing Binary Stars–Modeling and Analysis (Springer-Verlag). DOI
Kurucz, R.L., 1979, *ApJS*, **40**, 1 DOI
Kwee, K.K. and Woerden, H., 1956, *BAN*, **12**, 327
Nelson, R.H., 2010, "Spectroscopy for Eclipsing Binary Analysis" in The Alt-Az Initiative, Telescope Mirror & Instrument Developments (Collins Foundation Press, Santa Margarita, CA), R.M. Genet, J.M. Johnson and V. Wallen (eds)

Nelson, R.H., 2013, Software by Bob Nelson,
`https://www.variablestarssouth.org/bob-nelson/`
Nelson, R.H., 2014, Spreadsheets, by Bob Nelson,
`https://www.variablestarssouth.org/bob-nelson/`
Nelson, R.H., Şenavci, H.V., Baştürk, Ö, and Bahar, E., 2014, *NewA*, **29**, 57 DOI
Nelson, R.H., Terrell, D., Milone, E.F., 2014, *NewAR*, **59**, 1 DOI
Nelson, R.H., Terrell, D., Milone, E.F., 2015, *NewAR*, **69**, 1 DOI
Nelson, R.H., Terrell, D., Milone, E.F., 2016, *NewAR*, **70**, 1 DOI
Nelson, R.H., 2016, Bob Nelson's O–C Files,
`http://www.aavso.org/bob-nelsons-o-c-files`
O–C Gateway, Paschke, A., `http://var2.astro.cz/ocgate/`
Rucinski, S. M., 2004, *IAUS*, **215**, 17
Terrell, D., 1994, Van Hamme Limb Darkening Tables, vers. 1.1.
Van Hamme, W., 1993, *AJ*, **106**, 2096 DOI
Whitney, B.S., 1959, *AJ*, **64**, 258 DOI
Wilson, R.E., and Devinney, E.J., 1971, *ApJ*, **166**, 605 DOI
Wilson, R.E., 1990, *ApJ*, **356**, 613 DOI
Wilson, R.E., 1998, Documentation of Eclipsing Binary Computer Model (available from the author)